Ras signaling promotes simultaneously and independently [fig. S1L (*7*)] three effects: activation of *al* and *dlim1* at the very center, activation of *Bar* in nearby cells, and repression of *bab* from the whole area. Regarding tarsal segments 1 to 4, *vn* acts as the repressory element working in parallel to *dac* to restrict the activation of *rn* and *bab* to the middle of the *Dll* domain. Tarsal segments 1 to 4 are thus defined in those *Dll*-expressing cells not simultaneously exposed to either the *dac* protein or EGFR-Ras signaling triggered by *vn* (Fig. 4 and fig. S1E).

Thus, interactions between genes and signals expressed in PD domains constitute a patterning mechanism for the development of new PD fates. We suspect that further PD interactions exist in *Drosophila* legs, for example, during trochanter development proximal to the *dac* domain (*7*).

The *Drosophila* tarsus develops in the absence of homeotic genes, suggesting that it is an ancestral ground-state limb structure (*15*). Because tarsal development is driven by PD interactions, altogether these results might suggest that these interactions are an ancestral process, possibly to be found in other animals. In primitive insect limbs, a transition in *dpp* expression (*16*, *17*) signals a *wg*- and *dpp*-independent patterning phase, whereas the conserved expression of *Dll*, *dac*, and *al* suggests a conservation of their functional roles (*18*). In vertebrate limbs, expression and requirements of *Dll*, *dac*, and *al* homologs are similar to those of insects (*19*–*21*), and experimental embryology has shown that insect and vertebrate limbs react to PD axis alterations in the same way (*22*).

Further work is required to clarify these issues and to obtain a complete understanding of PD patterning in animal appendages. Our results show the importance of an element whose role had long been suspected (*1*, *22*), that is, the existence of PD interactions that complete the initial PD organization generated by dorsal-ventral and anterior-posterior patterning cascades.

References and Notes

1. G. Campbell, T. Weaver, A. Tomlinson, *Cell* **74**, 1113 (1993).
2. J. P. Couso, M. Bate, A. Martinez-Arias, *Science* **259**, 484 (1993).
3. J. Jiang, G. Struhl, *Cell* **86**, 401 (1996).
4. F. Diaz-Benjumea, B. Cohen, S. Cohen, *Nature* **372**, 175 (1994).
5. T. Lecuit, S. Cohen, *Nature* **388**, 139 (1997).
6. J. P. Couso, S. A. Bishop, *Int. J. Dev. Biol.* **42**, 345 (1998).
7. Materials and methods and other supplementary material are available on *Science* Online.
8. J. Castelli-Gair, M. Akam, *Development* **121**, 2973 (1995).
9. S. E. St Pierre, M. I. Galindo, J. P. Couso, S. Thor, *Development* **129**, 1273 (2002).
10. D. Godt, J. Couderc, S. Cramton, F. Laski, *Development* **119**, 799 (1993).
11. B. Schnepp, G. Grumbling, T. Donaldson, A. Simcox, *Genes Dev.* **10**, 2302 (1996).
12. R. Schweitzer, B. Shilo, *Trends Genet.* **13**, 191 (1997).
13. J. I. Pueyo, M. I. Galindo, S. A. Bishop, J. P. Couso, *Development* **127**, 5391 (2000).
14. T. Kojima, M. Sato, K. Saigo, *Development* **127**, 769 (2000).
15. F. Casares, R. S. Mann, *Science* **293**, 1477 (2001).
16. E. Jockusch, C. Nulsen, S. Newfeld, L. Nagy, *Development* **127**, 1617 (2000).
17. N. Niwa *et al.*, *Development* **127**, 4373 (2000).
18. A. Abzhanov, T. C. Kaufman, *Dev. Biol.* **227**, 673 (2000).
19. R. Robledo, L. Rajan, X. Li, T. Lufkin, *Genes Dev.* **16**, 1089 (2002).
20. R. J. Davis, W. Shen, T. A. Heanue, G. Mardon, *Dev. Genes Evol.* **209**, 526 (1999).
21. S. Qu *et al.*, *Development* **125**, 2711 (1998).
22. S. V. Bryant, V. French, P. J. Bryant, *Science* **212**, 993 (1981).

23. We thank A. Simcox and G. Campbell for unpublished results and discussions on EGFR signaling, C. Sainsot for technical assistance, and I. Pueyo, F. Casares, and J. Bacon for manuscript comments. This work was supported by the Wellcome and Leverhulme Trusts.

Supporting Online Material

www.sciencemag.org/cgi/content/full/297/5579/256/DC1
Materials and Methods
Supporting Text
Fig. S1

28 March 2002; accepted 13 June 2002

Mediation of Poly(ADP-Ribose) Polymerase-1–Dependent Cell Death by Apoptosis-Inducing Factor

Seong-Woon Yu,[1]* Hongmin Wang,[1]* Marc F. Poitras,[1] Carmen Coombs,[1] William J. Bowers,[5] Howard J. Federoff,[5] Guy G. Poirier,[6] Ted M. Dawson,[1,2,4] Valina L. Dawson[1,2,3,4]†

Poly(ADP-ribose) polymerase-1 (PARP-1) protects the genome by functioning in the DNA damage surveillance network. PARP-1 is also a mediator of cell death after ischemia-reperfusion injury, glutamate excitotoxicity, and various inflammatory processes. We show that PARP-1 activation is required for translocation of apoptosis-inducing factor (AIF) from the mitochondria to the nucleus and that AIF is necessary for PARP-1–dependent cell death. *N*-methyl-*N*′-nitro-*N*-nitrosoguanidine, H_2O_2, and *N*-methyl-D-aspartate induce AIF translocation and cell death, which is prevented by PARP inhibitors or genetic knockout of PARP-1, but is caspase independent. Microinjection of an antibody to AIF protects against PARP-1–dependent cytotoxicity. These data support a model in which PARP-1 activation signals AIF release from mitochondria, resulting in a caspase-independent pathway of programmed cell death.

PARP-1 is a nuclear enzyme that responds to DNA damage and facilitates DNA repair (*1*–*3*). Once activated, PARP-1 transfers 50 to 200 molecules of ADP-ribose to a variety of nuclear proteins, including histones and PARP-1 itself (*1*–*4*). PARP-1 activation mediates cell death in ischemia-reperfusion injury after cerebral ischemia (*5*, *6*) and myocardial infarction (*7*), inflammatory injury, reactive oxygen species-induced injury (*8*), glutamate excitotoxocity (*9*, *10*), and 1-methyl-4-phenyl-1,2,3,6-tetrahydropyridine (MPTP) injury (*11*, *12*). The molecular mechanisms of PARP-1–induced cell death are not known, although one possibility is that PARP-1 signals to downstream cell death effectors.

To examine the mechanism by which PARP-1 activation kills cells, immortalized mouse embryonic fibroblasts from wild-type and PARP-1–knockout (KO) mice (*13*) were exposed to *N*-methyl-*N*′-nitro-*N*-nitrosoguanidine (MNNG), a DNA-alkylating agent that potently activates PARP-1 and elicits PARP-1–dependent cytotoxicity. Exposure to 0.5 mM MNNG for 15 min induces nearly complete cell death in wild-type fibroblasts within 12 to 24 hours, whereas PARP-1–KO fibroblasts are resistant to the toxic effects of MNNG (Fig. 1A). PARP-1 activation consumes nicotinamide adenine dinucleotide (NAD^+) through the adenosine 5′-diphosphate (ADP)-ribosylation of nuclear associated proteins (*8*), resulting in an 80% reduction of NAD^+ levels within 15 min in wild-type fibroblasts (Fig. 1B). By 30 min, NAD^+ levels are no longer detectable. In contrast, NAD^+ levels in PARP-1–KO fibroblasts are maintained to greater than 60% of control values for up to 24 hours (Fig. 1B). The broad-spectrum caspase inhibitors, boc-as-

[1]Departments of Neurology, [2]Neuroscience, and [3]Physiology; and [4]the Institute for Cell Engineering, Johns Hopkins University School of Medicine, Baltimore, MD 21287, USA. [5]Department of Neurology, Center for Aging and Developmental Biology, University of Rochester, NY 14642, USA. [6]Health and Environment Unit, Laval University Medical Research Center, CHUQ, Ste-Foy, Quebec G1V 4G2, Canada.

*These authors contributed equally to this work.
†To whom correspondence should be addressed. E-mail: vdawson@jhmi.edu

partyl-fmk (BAF) (100 μM) and Z-VAD.fmk (100 μM), fail to block MNNG-induced toxicity (Fig. 1C) but effectively inhibit caspase activation (fig. S1). In contrast, the specific PARP inhibitors, 1,5-dihydroxyisoquinoline (DHIQ) (300 μM) and 3,4-dihydro-5-[4-(1-piperidinyl)butoxy]-1(2H)-isoquinolinone (DPQ) (30 μM), completely block MNNG-induced toxicity (Fig. 1C). PARP-1–KO fibroblasts are also resistant to MNNG-induced cell death (Fig. 1C). Taken together, these data indicate that MNNG-mediated cell death is PARP-1 dependent and caspase independent.

We next examined whether PARP-1–mediated cell death involved apoptosis-inducing factor (AIF), because AIF-induced cell death is also caspase independent (*14*, *15*). AIF is a mitochondrial flavoprotein that is released in response to death stimuli (*16*). Confocal microscopy and subcellular fractionation reveal AIF translocation into the nucleus in wild-type, but not in PARP-1–KO fibroblasts, after treatment with MNNG (Fig. 1, D and E). In addition, inhibition of PARP by DPQ in wild-type fibroblasts ameliorates the nuclear condensation and AIF translocation seen after MNNG treatment (Fig. 1, D and E). These observations implicate PARP-1 activation in triggering AIF translocation.

To determine whether these findings extend to other forms of PARP-1–dependent cell death, fibrobast cultures were exposed to H_2O_2, which induces oxidative stress leading to DNA damage and PARP-1 activation (*17*–*19*). H_2O_2 also induces AIF translocation and cell death in a PARP-1–dependent, but caspase-independent manner (fig. S2, A to D).

We then investigated whether these findings extend to the central nervous system by evaluating *N*-methyl-D-aspartate (NMDA) glutamate receptor-mediated toxicity in cortical neurons. NMDA neurotoxicity plays a prominent role in neuronal damage after stroke and neurodegenerative disorders (*20*), in part through activation of PARP-1 (*6*, *9*, *10*). A 5-min application of NMDA (500 μM) induces robust activation of PARP-1 in cortical cultures from wild-type animals, whereas NMDA-receptor stimulation fails to activate poly(ADP-ribose) (PAR) polymer formation in PARP-1–KO cortical cultures (Fig. 2A) (*10*). Similarly, NMDA-receptor stimulation induces nuclear condensation and AIF translocation in wild-type cortical cultures, but fails to elicit nuclear condensation and AIF translocation in PARP-1–KO cortical cultures (Fig. 2, B and C). As previously reported, NMDA receptor stimulation kills the majority of wild-type cortical neurons, but NMDA fails to kill PARP-1–KO cultures or wild-type cultures treated with DPQ (*6*) (Fig. 2D). The broad-spectrum caspase inhibitor, Z-VAD.fmk, has no protective effect against NMDA neurotoxicity and fails to block AIF translocation and nuclear condensation in cortical cultures (Fig. 2D). Similar results are obtained when assessing cell death by Hoechst 33342 and propidium iodide staining (*21*). These results taken together suggest that NMDA-receptor stimulation causes AIF translocation in a caspase-independent, but PARP-1–dependent, fashion and that NMDA-mediated cell death may be linked to AIF translocation.

When AIF translocates to nuclei, it leads to chromatin condensation and triggers phosphatidylserine exposure on the cell surface and mitochondrial membrane depolarization (*14*). To clarify the cellular consequences of AIF release, cyt *c*, mitochondrial membrane

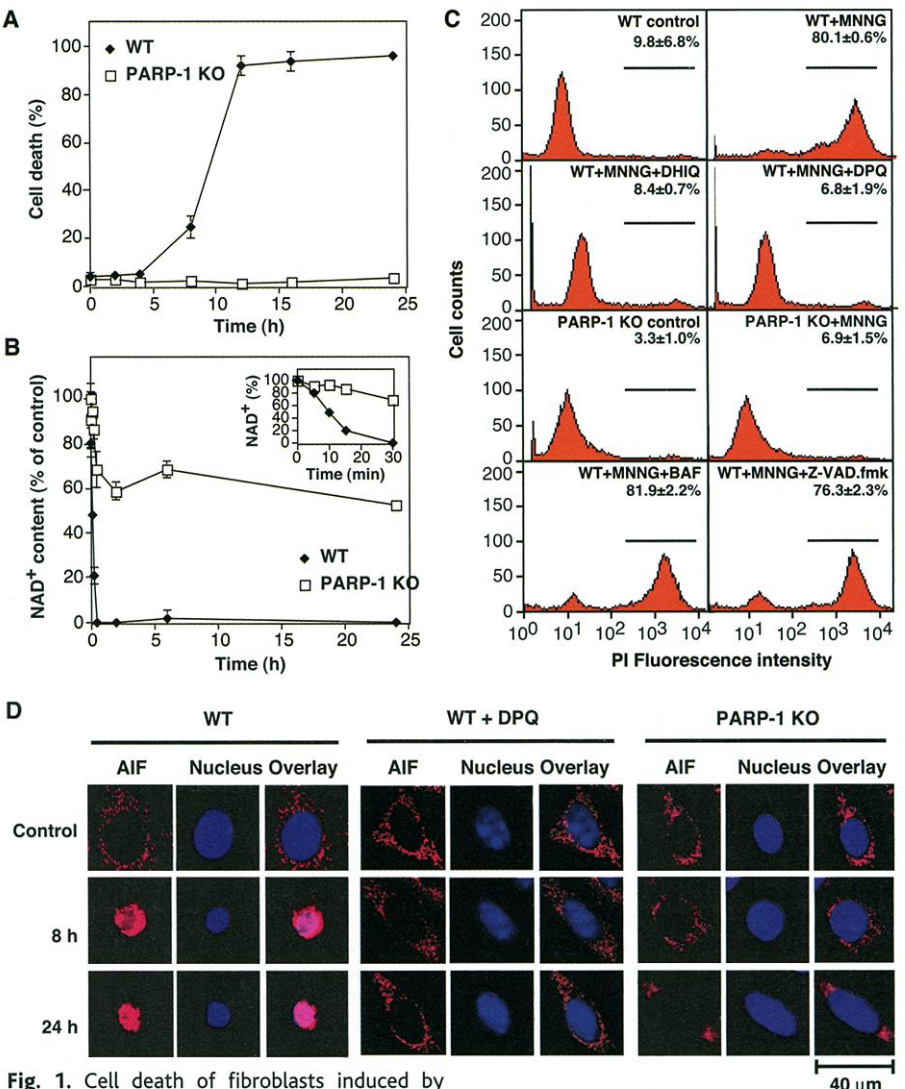

Fig. 1. Cell death of fibroblasts induced by MNNG is PARP-1 dependent but caspase independent. (**A**) Flow cytometry analysis of fibroblasts exposed to MNNG (0.5 mM, 15 min). (**B**) Time-course analysis of the depletion of cellular NAD^+ level in fibroblasts after MNNG treatment. (**C**) Flow cytometry analysis of MNNG-induced cell death in the presence of either PARP inhibitors [DHIQ (300 μM) and DPQ (30 μM)] or pan-caspase inhibitors [Z-VAD.fmk (100 μM) or BAF (100 μM)]. (A) to (C) Numbers are mean values of three independent experiments ±SD. (**D**) The translocation of AIF in MNNG-treated fibroblasts is PARP-1 dependent. The redistribution of AIF into the nuclei is demonstrated by the overlap of AIF and nuclear staining, as denoted by the pink color. (**E**) Analysis of AIF translocation by subcellular fractionation. The fibroblasts 8 hours after MNNG treatment (MNNG) or control cells (C) were subjected to subcellular fractionation, and immunoblotting was performed with nuclear (N) and mitochondrial (M) fractions. Histone and manganese superoxide dismutase (MnSOD) were used as nuclear and mitochondrial marker proteins, respectively. The experiments in (D) and (E) were repeated at least three times with similar results.

depolarization and annexin-V staining were monitored (*22*) (Fig. 3 and fig. S3). AIF translocation to the nucleus is detectable within 5 to 15 min of MNNG treatment of wild-type fibroblasts (Fig. 3, A and B, and fig. S3A), as is nuclear condensation and annexin-V–positive staining. Mitochondrial membrane potential (*23*) begins to dissipate within 15 min after MNNG treatment and is completely absent within 1 hour (Fig. 3, A and B). In contrast, cyt *c* dissipates much later, 1 to 2 hours after MNNG treatment (Fig. 3, A and B, and fig. S3B). Activated caspase-3 fragments are detectable after 2 hours of MNNG treatment of wild-type fibroblasts paralleling the detection of cyt *c* in the cytosolic fraction and the observation of PARP-1 cleavage within the nuclear fraction (fig. S3A). Active caspase-3 and cyt *c* release are not detected in the PARP-1–KO fibroblasts after MNNG treatment (Fig. 3C and

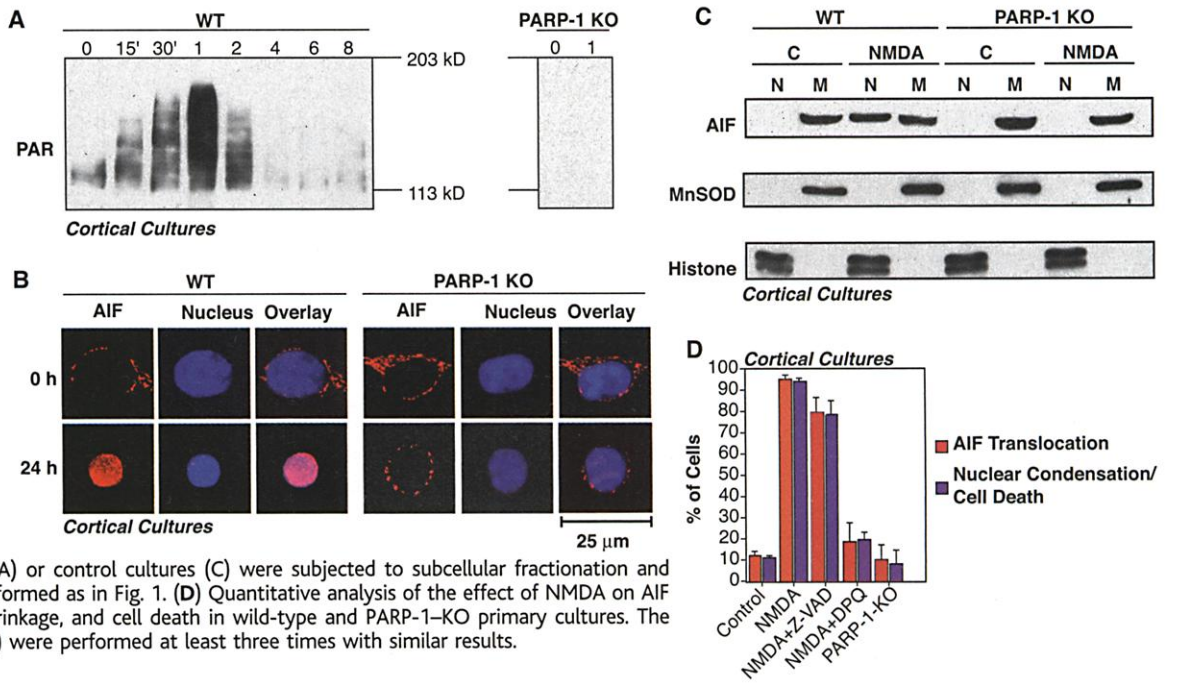

Fig. 2. NMDA (500 μM) induces cell death and AIF translocation in a PARP-1–dependent manner. (**A**) The time course of NMDA-induced PARP-1 activation in primary cortical cultures, as detected by Western blot analysis with an antibody to PAR. (**B**) Representative confocal images of the effect of NMDA on AIF translocation and nuclear shrinkage in wild-type and PARP-1–KO neurons. (**C**) Analysis of AIF translocation by subcellular fractionation. The primary cultures 6 hours after NMDA treatment (NMDA) or control cultures (C) were subjected to subcellular fractionation and immunoblotting was performed as in Fig. 1. (**D**) Quantitative analysis of the effect of NMDA on AIF translocation, nuclear shrinkage, and cell death in wild-type and PARP-1–KO primary cultures. The experiments in (A) to (D) were performed at least three times with similar results.

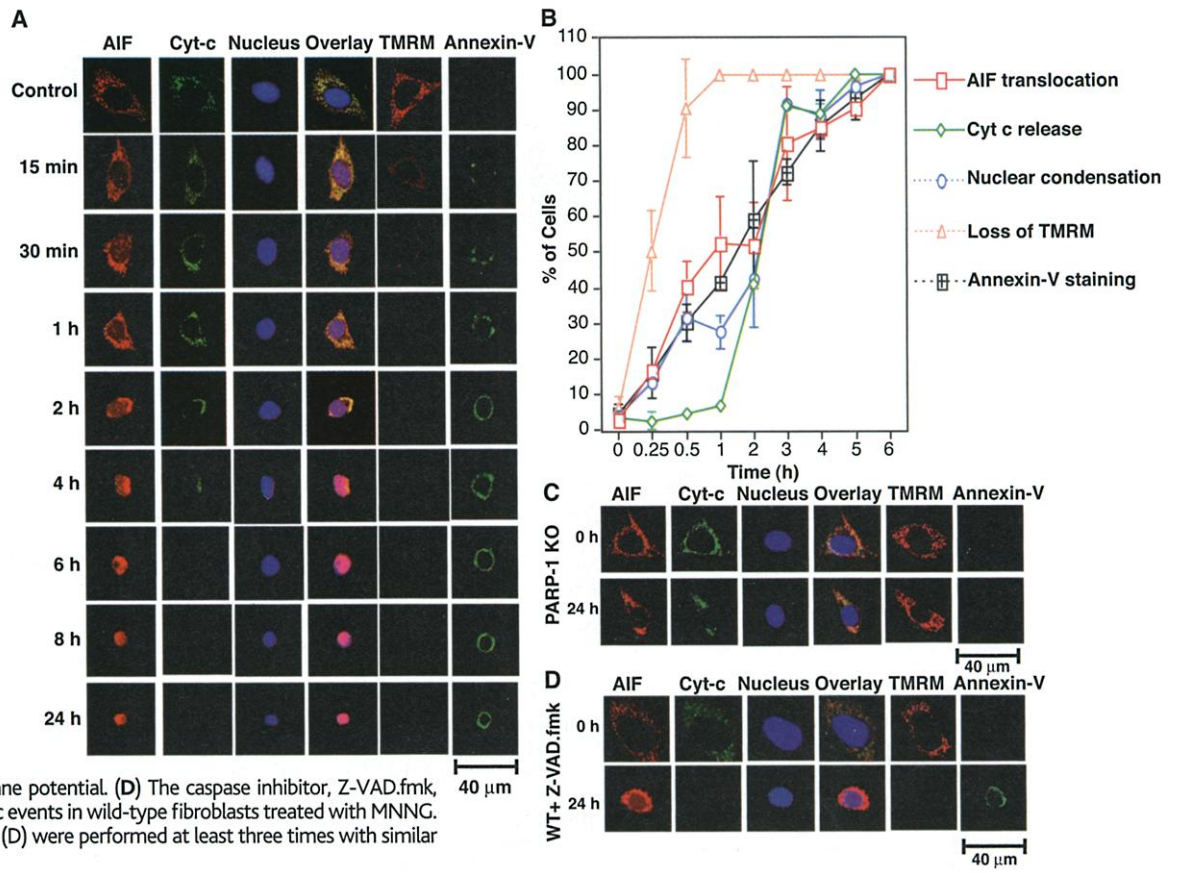

Fig. 3. Analysis of the apoptotic events in MNNG-treated fibroblasts. Representative confocal images (**A**) and quantitative analysis of apoptotic events (**B**) in wild-type fibroblasts after MNNG treatment. The overlay represents the fusion image of red (AIF), green (cyt *c*), and blue (nucleus) fluorescence. Yellow reflects the colocalization of AIF and cyt *c* in the mitochondria. Pink reflects AIF translocation into the nucleus. Note the rapid staining of annexin-V (green) and loss of mitochondrial membrane potential (represented by the loss of red fluorescence of TMRM). (**C**) PARP-1–KO fibroblasts are resistant to MNNG treatment, and AIF and cyt *c* are retained in the mitochondria without annexin-V staining or loss of mitochondrial membrane potential. (**D**) The caspase inhibitor, Z-VAD.fmk, fails to block the apoptotic events in wild-type fibroblasts treated with MNNG. The experiments in (A) to (D) were performed at least three times with similar results.

fig. S3), and PARP-1–KO fibroblasts maintain the punctate immunostaining pattern of AIF and cyt *c*, indicating that these pro-death factors still reside in the mitochondria (Fig. 3C). Mitochondrial membrane potential is not reduced (Fig. 3C) and annexin-V staining is not observed in PARP-1–KO fibroblasts (Fig. 3C). The broad-spectrum caspase inhibitor *Z*-VAD.fmk (100 μM) blocks caspase activation (fig. S1), but it does not prevent AIF translocation, nuclear condensation, annexin-V staining, or dissipation of the mitochondrial membrane potential in MNNG-treated wild-type fibroblasts (Fig. 3D), which is consistent with the lack of protection (Fig. 1C). These results suggest that MNNG-induced cell death and the appearance of cell death markers are mediated by PARP-1 activation and may be induced by AIF through caspase independent-mechanisms. Subcellular fractionation studies with a more detailed time course confirm that PARP-1 activation and AIF translocation markedly precedes the appearance of biochemical markers of apoptosis (fig. S3).

Because the release of AIF from the mitochondria can be prevented by overexpression of bcl-2 (*14*), the effect of forced overexpression of bcl-2 was investigated. Bcl-2 overexpression retards AIF translocation and nuclear shrinkage up to 2 hours after MNNG treatment but fails to prevent AIF translocation or nuclear shrinkage at 24 hours (fig. S4). Thus, the release of AIF induced by MNNG treatment of fibroblasts is delayed by bcl-2 overexpression, which is consistent with prior reports that bcl-2 can block AIF release. However, bcl-2 alone is not sufficient to prevent MNNG-induced AIF release and cell death. To determine what role AIF translocation might play in PARP-1–dependent cell death, a neutralizing antibody to AIF was microinjected (*24*) into wild-type fibroblasts before MNNG treatment (Fig. 4). Microinjection of anti-AIF antibody prevents nuclear condensation (Fig. 4A) and provides greater then 60% protection at 6 and 24 hours against MNNG cytotoxicity in wild-type fibroblasts (Fig. 4B), whereas injection of rabbit IgG fails to protect fibroblasts from MNNG-induced cell death. Microinjecting an antibody to poly(ADP-ribose) glycohydrolase that was affinity purified and prepared in a similar manner to the AIF antibody also fails to protect fibroblasts from MNNG-induced cell death (*21*). The maintenance of nuclear integrity and the cytoprotection by neutralizing AIF antibody is reversed by co-injecting the AIF antibody with AIF peptides (Fig. 4, A and B), confirming the importance of AIF translocation in PARP-1–dependent cell death. To investigate the specificity of the cytoprotective effects of the neutralizing AIF antibody and to ensure that it was not nonselectively blocking other forms of cell death, we treated microinjected fibroblasts with TNFα, a cytokine that induces robust caspase-dependent cell death (*25*). Antibodies to AIF are unable to protect fibroblasts from nuclear condensation and cell death after exposure to TNFα (Fig. 4, C and D). Western blot analysis confirms immunodepletion of AIF by the AIF antibody and efficacy of peptide blockade (Fig. 4E). Taken together, these results indicate that AIF is an essential downstream effector of PARP-1–initiated cell death.

Our data indicate that PARP-1 activation is required for AIF translocation during cell death initiated by MNNG and H_2O_2 in fibroblasts and NMDA in cortical neurons. Moreover, AIF appears to be essential for PARP-1–mediated cell death. Although PARP-1–dependent cell death is thought to be necrotic (*3*, *8*, *26*, *27*), our findings suggest that PARP-1–mediated cell death also has many features in common with apoptotic forms of cell death.

PARP-1–mediated cell death has been proposed to be due, in part, to NAD^+ consumption and subsequent energy depletion (*26*, *27*). Decrements in NAD^+ appear to parallel AIF translocation, nuclear condensation, annexin-V staining, and mitochondrial membrane depolarization. NAD^+ decrements are coincident with PARP-1 activation, thereby temporally linking PARP-1 activation,

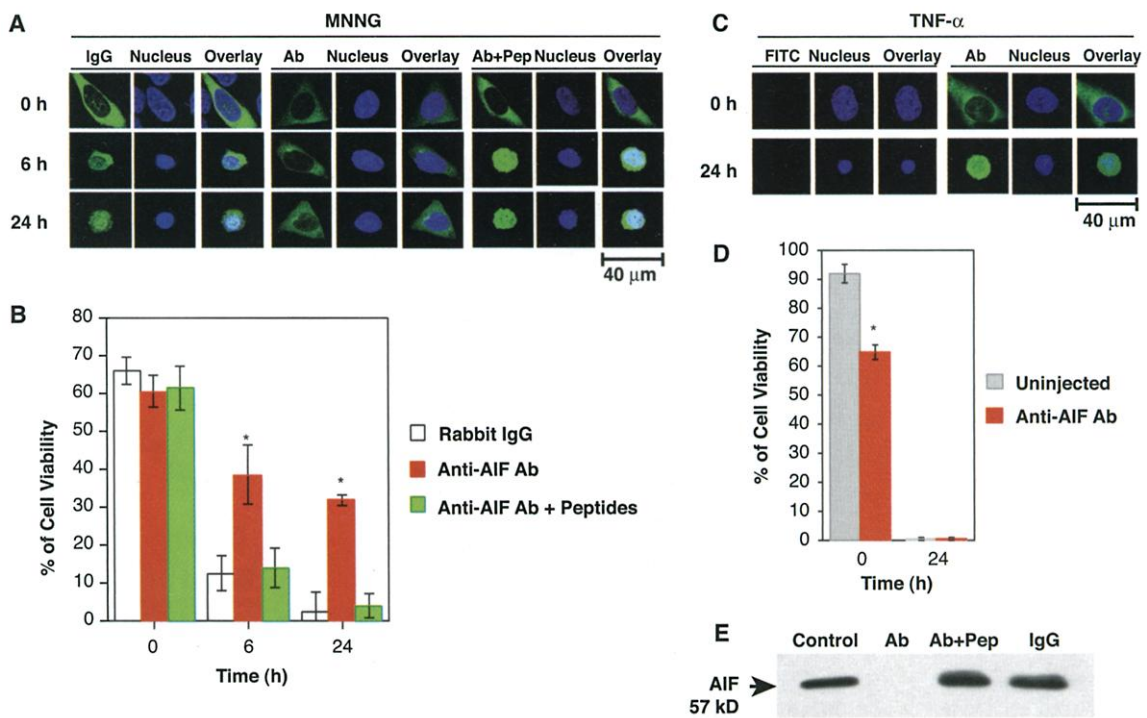

Fig. 4. Microinjection of antibodies to AIF protects cells from MNNG-induced cell death, but not TNFα. (**A**) In the left and right panels respectively, fibroblasts were injected with rabbit IgG or antibodies to AIF plus the immunogenic peptides (amino acids 151 to 170 and 181 to 200). Cell shrinkage and nuclear condensation indicative of cell death can be seen at both 6 and 24 hours after MNNG (500 μM) treatment. In the middle panel, fibroblasts were injected with purified antibodies to AIF. Normal morphology of cells and nuclei is observed in the majority of microinjected cells at both 6 and 24 hours after MNNG treatment. (**B**) Cell viability after microinjection of antibodies to AIF and MNNG treatment. Cells were scored as either dead or alive based on their shapes and nuclear and cytosolic morphology. (**C**) Uninjected cells (left panel) or cells microinjected with antibodies to AIF (right panel) were incubated with TNFα for 24 hours. Antibodies to AIF fail to prevent cell shrinkage and nuclear condensation. (**D**) Cell viability after microinjection of antibodies to AIF and TNFα treatment. (**E**) AIF in the mitochondrial extracts was neutralized by antibodies to AIF. Competition with peptide antigens or rabbit IgG did not immunodeplete AIF. Control signifies the starting mitochondrial fraction obtained from the mouse liver mitochondria. The experiments in (A) to (E) were performed at least three times with similar results. Data are expressed as the means ±SD. Significance was determined by a one-way analysis of variance with a student's *t* test, $^*P < 0.05$.

NAD^+ levels, and AIF translocation. The rescue of cells from PARP-1–mediated cell death by blocking AIF function with antibodies to AIF suggests that NAD^+ consumption and subsequent energy depletion may not be sufficient for PARP-1–mediated cell death. Instead, NAD^+ consumption and subsequent energy depletion may act as a signal that initiates the death program through AIF translocation. When mitochondria are isolated in NAD^+-free buffer, AIF is not released, suggesting that loss of cytosolic NAD^+ is not sufficient to trigger the release of AIF from mitochondria (*21*). The NAD^+ pool is largely compartmentalized within the mitochondria (*28*), where depletion of NAD^+ due to PARP-1 activation might be expected to cause alterations in the mitochondria (*29*) and signal the release of AIF.

Based on the observations reported here, we propose that PARP-1 activation elicited by DNA damage leads to a decrement in NAD^+ that is perceived by the mitochondria. Cytosolic AIF translocates to the nucleus and initiates nuclear condensation (*14*). Once the nucleus condenses, the cell is doomed to die, because large-scale chromatin fragmentation usually accompanies nuclear condensation (*14*). Additionally, cytosolic AIF acts on the mitochondria to collapse the mitochondrial membrane potential and initiates the release of cyt *c*, which activates caspases (*14*). The late activation of caspases after the executioner step of AIF release may facilitate the dissolution of the cell. However, caspase activation is not required for cell death, because caspase inhibitors cannot rescue the cell from PARP-1–initiated cell death.

References and Notes

1. D. Lautier, J. Lagueux, J. Thibodeau, L. Menard, G. G. Poirier, *Mol. Cell. Biochem.* **122**, 171 (1993).
2. G. de Murcia *et al.*, *Mol. Cell. Biochem.* **138**, 15 (1994).
3. S. Shall, G. de Murcia, *Mutat. Res.* **460**, 1 (2000).
4. M. E. Smulson *et al.*, *Adv. Enzyme Regul.* **40**, 183 (2000).
5. M. Endres, Z. Q. Wang, S. Namura, C. Waeber, M. A. Moskowitz, *J. Cereb. Blood Flow Metab.* **17**, 1143 (1997).
6. M. J. Eliasson *et al.*, *Nature Med.* **3**, 1089 (1997).
7. A. A. Pieper *et al.*, *Mol. Med.* **6**, 271 (2000).
8. C. Szabo, V. L. Dawson, *Trends Pharmacol. Sci.* **19**, 287 (1998).
9. J. Zhang, V. L. Dawson, T. M. Dawson, S. H. Snyder, *Science* **263**, 687 (1994).
10. A. S. Mandir *et al.*, *J. Neurosci.* **20**, 8005 (2000).
11. A. S. Mandir *et al.*, *Proc. Natl. Acad. Sci. U.S.A.* **96**, 5774 (1999).
12. C. Cosi, M. Marien, *Ann. N.Y. Acad. Sci.* **890**, 227 (1999).
13. Z. Q. Wang *et al.*, *Genes Dev.* **11**, 2347 (1997).
14. S. A. Susin *et al.*, *Nature* **397**, 441 (1999).
15. G. Kroemer, J. C. Reed, *Nature Med.* **6**, 513 (2000).
16. N. Joza *et al.*, *Nature* **410**, 549 (2001).
17. Y. J. Lee, E. Shacter, *J. Biol. Chem.* **274**, 19792 (1999).
18. D. M. Filipovic, X. Meng, W. B. Reeves, *Am. J. Physiol.* **277**, F428 (1999).
19. J. A. Walisser, R. L. Thies, *Exp. Cell Res.* **251**, 401 (1999).
20. B. Meldrum, J. Garthwaite, *Trends Pharmacol. Sci.* **11**, 379 (1990).
21. S.-W. Yu, H. Wang, M. F. Poitras, T. M. Dawson, V. L. Dawson, data not shown.
22. I. Vermes, C. Haanen, H. Steffens-Nakken, C. Reutelingsperger, *J. Immunol. Methods* **184**, 39 (1995).
23. V. Petronilli, D. Penzo, L. Scorrano, P. Bernardi, F. Di Lisa, *J. Biol. Chem.* **276**, 12030 (2001).
24. K. F. Ferri *et al.*, *J. Exp. Med.* **192**, 1081 (2000).
25. P. C. Rath, B. B. Aggarwal, *J. Clin. Immunol.* **19**, 350 (1999).
26. Z. Herceg, Z. Q. Wang, *Mol. Cell. Biol.* **19**, 5124 (1999).
27. H. C. Ha, S. H. Snyder, *Proc. Natl. Acad. Sci. U.S.A.* **96**, 13978 (1999).
28. F. Di Lisa, R. Menabo, M. Canton, M. Barile, P. Bernardi, *J. Biol. Chem.* **276**, 2571 (2001).
29. L. Virag, A. L. Salzman, C. Szabo, *J. Immunol.* **161**, 3753 (1998).

30. We thank W. Cotman for secretarial assistance and D. Ginty and M. Hardwick for their helpful comments. Supported by grants from the NIH, the Center for ALS Research at Johns Hopkins Medical Institutions, the American Heart Association, and the Mary Lou McIlhaney Scholar Award. Under an agreement between the Johns Hopkins University and Guilford Pharmaceuticals, T.M.D. and V.L.D. are entitled to a share of sales royalty received by the university from Guilford. T.M.D. and the university also own Guilford stock, and the university stock is subject to certain restrictions under university policy. The terms of this arrangement are being managed by the university in accordance with its conflict-of-interest policies.

Supporting Online Material

www.sciencemag.org/cgi/content/full/297/5579/259/DC1
Materials and Methods
Figs. S1 to S4
References and Notes

7 March 2002; accepted 22 May 2002